Journal for Technology and Science
Homepage : https://journal.antispublisher.com/index.php/IPTEKS/index
Email : admin@antispublisher.com

e-ISSN : 3047-4337
JOTECH, Vol. 3, No. 3, July 2026
Page 104-115

Describe the Effect of High Temperatures on Certain General Properties of the Compound (MgO-Ni) at High Temperatures

Dheyab T. Noori
Tikrit University, Iraq

DOI : https://doi.org/10.61796/ipteks.v3i3.547

Sections Info

Article history:
Submitted: April 17, 2026
Final Revised: May 12, 2026
Accepted: June 07, 2026
Published: July 27, 2026

Keywords:
MgO-Ni Ceramic Composite
Self-Sintering
Calcination Temperature
Microstructure
Mechanical Properties

ABSTRACT

Objective: *In this research, the ceramic compound MgO-Ni was prepared and studied by the self-sintering method, with the study focusing on the effect of high temperatures on the crystal structure and some general properties.* ***Method:*** *In this research, the ceramic compound MgO-Ni was prepared and studied by the self-sintering method, with the study focusing on the effect of high temperatures on the crystal structure and some general properties.* ***Results:*** *The results obtained yielded important conclusions, as the scanning electron microscope image showed that the prepared compound possesses a homogeneous, microscopic crystalline structure. This is consistent with the X-ray diffraction analysis, which shows a regular grain distribution and the absence of cracks. This reflects the efficiency of the preparation and calcination methods. Furthermore, the scanning electron microscope (SEM) images showed that the grain size increases with rising temperatures. This behaviour is attributed to improved atomic diffusion, which is an excellent finding from an applied perspective. Furthermore, the mechanical results of the compound showed a marked improvement with increasing temperature, which is attributed to a decrease in porosity and an increase in intergranular cohesion. The increase in the magnesium oxide content also provided a significant basis for enhancing the compound's hardness, thanks to its hard ceramic nature. Additionally, the nickel mineral phase contributed to strengthening the structural bond and reducing the collapse of the h s, likewise, the compressive strength showed a marked increase, which indicates the stability of the composite's mechanical behaviour.* ***Novelty:*** *Finally, it can be concluded that the calcination temperature is a key factor in controlling the microstructure and improving the mechanical and physical properties of the composite without the need to alter its chemical composition. The results confirm that the prepared composite possesses high structural stability and excellent mechanical and thermal performance. making it suitable for engineering applications that require high-hardness materials.*

INTRODUCTION

Powers have diverse uses in the precision engineering industry and plumbing technologies [1]. Composites are a combination of two or more substances. Each of these substances has unique physical, chemical, and mechanical properties. This results in the production of a new substance whose properties are different from those of the individual substances used in the process [2], [3]. The new substance has properties that cannot be attained in other traditional substances such as polymers, metals, and ceramics. This substance formed by the combination of these materials is referred to as a composite material [4], [5]. The assessment of whether the composites can be used in an application depends to a great extent on their mechanical and physical properties [6]. Industrial development and increased requirements for substances that cannot be made using other means have resulted in the invention of the powder metallurgy process, which is basically the blending of ceramic substances with metal powders to make products with better characteristics [7], [8], [9], [10]. Powder metallurgy is carried out by preparing the

powder in order to know the size and shape of the particles and then mixing them in order to blend the powders as per the given ratio [11], [12], [13]. Compaction and then sintering of materials below the melting temperature of the matrix material take place after blending [14]. High temperatures are necessary during the production of composites based on metals and ceramics, thus creating the problems associated with the compatibility of the matrix and the reinforcing material [15, [16], [17], [18]. The issue of chemical compatibility is related to reactions taking place at the interface, and this might have an impact on the stability of the composite structure. These problems can be solved either by choosing a lower-temperature manufacturing process, e.g., powders, or by selecting thermodynamically stable phases. In contrast, the issue of mechanical compatibility is associated with thermal constants, especially the coefficients of thermal expansion of individual components, where their difference causes internal stress because of temperature changes, and it often occurs for fiber-reinforced composites. It can be avoided through the selection of matrices with high ductility or with a similar thermal expansion coefficient of the matrix and reinforcing phase. The final properties of metal-matrix composites depend on the interaction between the matrix and the reinforcing phase; their application at high temperatures could cause the diffusion of the internal phases into each other, which could lead to the weakening of the materials or the creation of new phases near the interface due to reactions of the matrix with the reinforcing phase. Such problems can be prevented by coating the reinforcing elements with materials that react with the matrix in a controlled manner, minimizing adverse effects. In the present study, nickel-Mg ferrite doped with aluminum has been produced chemically with ferric nitrate, nickel nitrate, and Mg nitrate along with aluminum nitrate. Technologies such as XRD and SEM are always used to characterize such nanomaterials [19], [20].

RESEARCH METHOD

The chemicals employed for sample synthesis in this research were varied as given in Table 1, for the synthesis of eleven samples of ferrite compounds according to the defined configuration through the sol-gel auto-combustion technique.

Table 1. Raw materials used in the preparation of the compound.

Sequence	Materials	Chemical formula	Purity	Weight ratio	Particle size	Density (g/cm^3)	The manufacturer
1	Magnesium oxide	MgO	99%	65%	Microbial	3.58	Sigma-Aldrich
2	Nickel	Ni	99%	35%	Microbial	8.90	Sigma-Aldrich

Auto-Combustion Method

The sample was prepared using the self-combustion method, whereby the resulting powder was placed in ceramic crucibles and calcined in an electric furnace at different temperatures (700,800,900, 100 and 1100 °C) for three hours at each temperature. This step aims to remove impurities and eliminate reaction by-products, such as water molecules, carbon dioxide, and other gases produced by the combustion process. The objective is to obtain purer nanoscale powders, which summarizes the stages of nanoscale ferrite formation. Following the sintering process, 1.1 g of the sintered samples at (700,800,900, 100, and 1100 °C) are taken and compressed into spherical pellets using a locally manufactured mould with a diameter of 10 mm and a thickness of 2 mm. This is achieved by applying a pressure of 4 tonnes for two minutes using a hydraulic press.

RESULTS AND DISCUSSION

Structural Characteristics

1. X-ray diffraction of the compound

The X-ray diffraction results showed in the Fig 1 that the compound synthesised by the self-combustion method exhibits a stable, two-phase crystalline structure within the angular range, with eight main diffraction peaks attributable to the Mg and Ni phases of the compound, which has a cubic crystal system (FCC) according to the International Standard Card for Mg oxide, numbered (00-100-0053) and the nickel data card (00-001-1260). The stability of the observed peak positions and the variation in their intensity reflect good regularity in the structural composition and a homogeneous distribution of the alloy's internal constituents, without the appearance of weak phases. Furthermore, calculations showed that the crystal size varies from one peak to another, which is considered normal behaviour in composite materials, as the crystal phase growth process depends on the direction of diffraction of the Miller indices (hkl), as well as the nature of the interaction between the Mg oxide and nickel phases. In the table 2 The crystal size values for all peaks ranged within the range (170–120) nanometres, which is considered approximately appropriate for a nanoscale size and indicates structural stability. When the results are considered in conjunction with the preparation conditions and method, it becomes clear that heat treatment during calcination plays an important role in controlling the crystal structure and improving the nanostructure and grain cohesion. An increase in temperature enhances the process of atomic diffusion and improves interparticle bonding whilst maintaining the stability of the crystal phases, thereby allowing precise control over the compositional properties of the material without compromising its homogeneity. These results are also significant for scientific applications, as they combine the chemical resistance with the good mechanical and thermal properties of all the compounds involved in the preparation process. These materials can be used in a wide range of applications, particularly those requiring wear and friction resistance, whilst components exposed to high temperatures are used in industrial control systems. In conclusion, it can be said that the high calcination temperatures involved in the preparation of this composite via the self-combustion

method lead to improved structural properties, thereby enhancing its suitability for engineering and industrial applications that require stable materials with reliable performance.

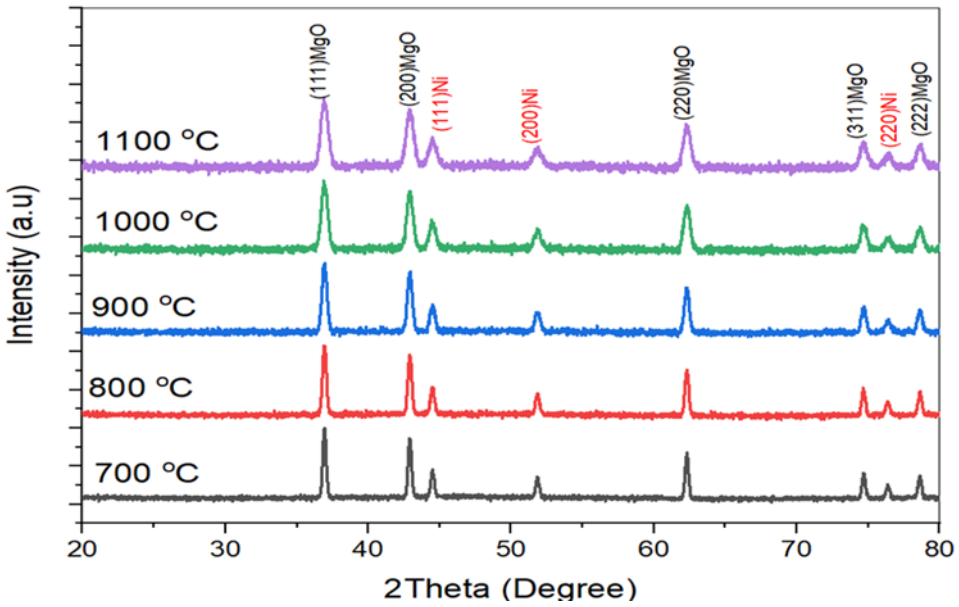

Figure 1. X-ray diffraction.

Table 2. X-ray diffraction results.

Sample T (oC)	2θ	FWHM	d (Å)	Size (nm)	hkl	Material
700 oC	36.93	0.0493	2.4321	170.0	111	MgO
	42.91	0.0514	2.1060	166.2	200	MgO
	44.50	0.0507	2.0343	169.2	111	Ni
	51.85	0.0533	1.7619	165.6	200	Ni
	62.30	0.0551	1.4891	168.6	220	MgO
	74.68	0.0606	1.2700	165.0	311	MgO
	76.38	0.0606	1.2459	166.9	220	Ni
	78.62	0.0613	1.2159	167.6	222	MgO
800 oC	**2θ**	**FWHM**	**d (Å)**	**Size (nm)**	**hkl**	**Material**
	36.93	0.0518	2.4321	162.5	111	MgO
	42.91	0.0547	2.1060	158.2	200	MgO
	44.50	0.0534	2.0343	161.2	111	Ni
	51.85	0.0561	1.7619	157.6	200	Ni
	62.30	0.0569	1.4891	160.6	220	MgO
	74.68	0.0633	1.2700	157.0	311	MgO
	76.38	0.0632	1.2459	158.9	220	Ni
	78.62	0.0641	1.2159	159.6	222	MgO
900 oC	**2θ**	**FWHM**	**d (Å)**	**Size (nm)**	**hkl**	**Material**
	36.93	0.0552	2.4321	152.5	111	MgO

	42.91	0.0583	2.1060	148.2	200	MgO
	44.50	0.0569	2.0343	151.2	111	Ni
	51.85	0.0601	1.7619	147.6	200	Ni
	62.30	0.0600	1.4891	150.6	220	MgO
	74.68	0.0669	1.2700	147.0	311	MgO
	76.38	0.0666	1.2459	148.9	220	Ni
	78.62	0.0676	1.2159	149.6	222	MgO
1000 oC	**2θ**	**FWHM**	**d (Å)**	**Size (nm)**	**hkl**	**Material**
	36.93	0.0601	2.4321	140.5	111	MgO
	42.91	0.0636	2.1060	136.2	200	MgO
	44.50	0.0616	2.0343	139.2	111	Ni
	51.85	0.0655	1.7619	135.6	200	Ni
	62.30	0.0648	1.4891	138.6	220	MgO
	74.68	0.0735	1.2700	135.0	311	MgO
	76.38	0.0727	1.2459	136.9	220	Ni
	78.62	0.0739	1.2159	137.6	222	MgO
1100 oC	**2θ**	**FWHM**	**d (Å)**	**Size (nm)**	**hkl**	**Material**
	36.93	0.0662	2.4321	127.5	111	MgO
	42.91	0.0702	2.1060	123.2	200	MgO
	44.50	0.0677	2.0343	126.2	111	Ni
	51.85	0.0725	1.7619	122.6	200	Ni
	62.30	0.0707	1.4891	125.6	220	MgO
	74.68	0.0812	1.2700	122.0	311	MgO
	76.38	0.0799	1.2459	123.9	220	Ni
	78.62	0.0813	1.2159	124.6	222	MgO

2. Scanning Electron Microscope (SEM)

Fig. (2) presents scanning electron microscope (SEM) micrographs of an MgO-Ni nanocomposite synthesized via the self-combustion approach, which displayed a homogeneous microstructure with uniform particle distribution and the clear absence of any agglomerations or surface cracks. Using the analysis of SEM micrographs, it was possible to determine the mean particle size, which was found in the range of 165.4 nm to 179.6 nm for various calcination temperatures, as depicted in Table 3. An increase in grain size is noticed with an increase in sintering temperature, which is a result of increased atomic diffusion and grain growth. Grain growth takes place at low temperatures, but it is not extensive owing to low atomic mobility at low temperatures. On the other hand, grain growth takes place at higher temperatures because of increased mobility of atoms in the grain boundaries, thus causing the smaller grains to join and form large grains. However, grain growth is moderate. It is desired from a practical point of view since it aids in preserving the homogeneity of the microstructure and ensuring a balance between mechanical strength and structural stability of the composite. Moreover,

the results obtained from SEM are consistent with those obtained from XRD analysis because the average size of grains in this range means a stable and strong structure, which has a positive effect not only on the physical but also on the mechanical properties of the material, including hardness and wear resistance. Therefore, it can be concluded that the degree of sintering control has a significant effect on the microstructure and properties of the MgO-Ni composite.

Table 3. Scanning electron microscope results.

The temperature (°C)	Crestal size (nm)
700	165.4
800	168.1
900	172.3
1000	174.8
1100	179.6

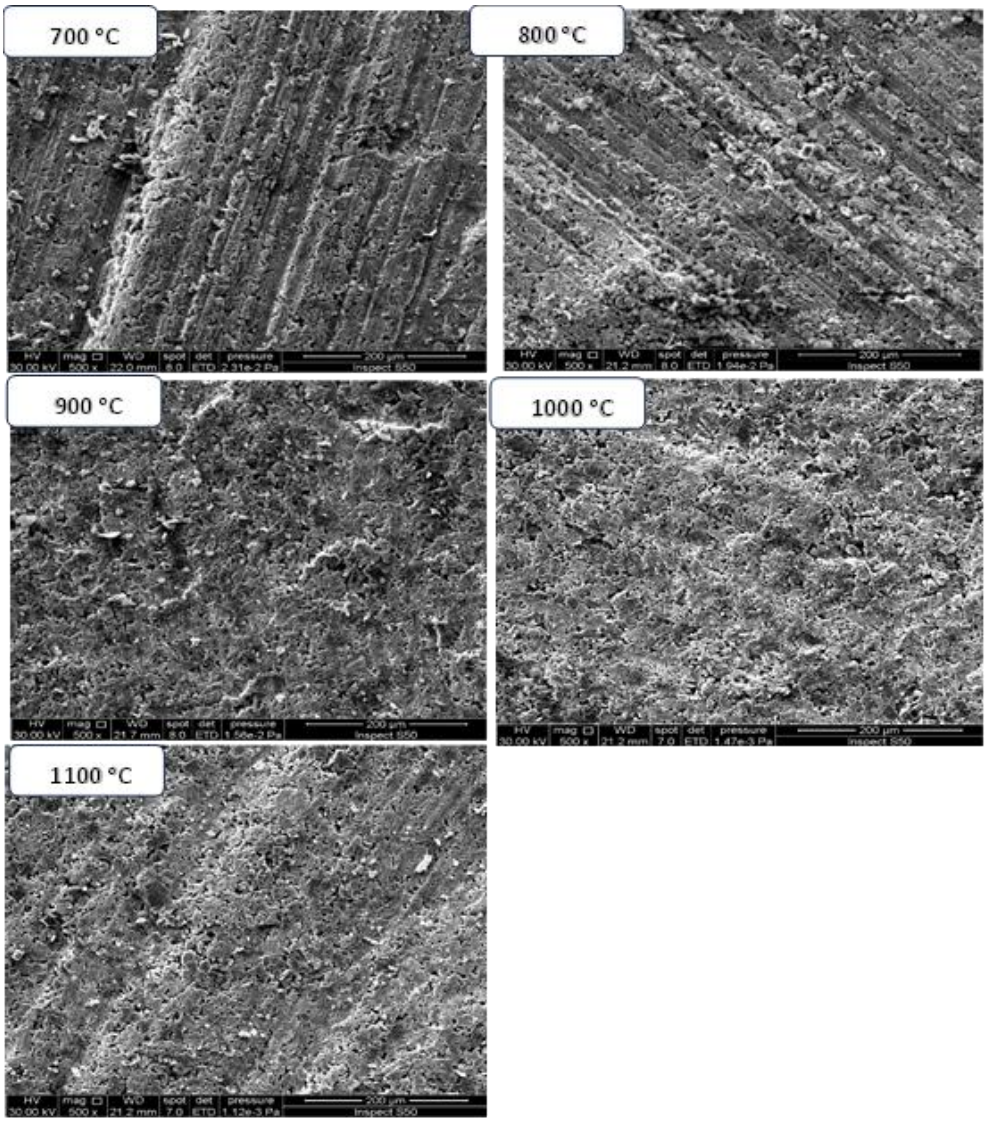

Figure 2. Scanning electron microscope images of the prepared compound.

Mechanical Properties

1. Vickers Hardness of the Composite

From the Vickers hardness results of the sample of the prepared and sintered composite in the range of 700–1100 °C as shown in Figure (3) and Table (4), it is evident that there was a definite improvement in the hardness value from 301.7 HV to 367.8 HV from 700 °C to 1100 °C, respectively. This improvement is a consequence of the influence of sintering on the microstructure of the composite, where an increase in the sintering temperature causes more atomic diffusion and thus more interparticle bonding. This gives rise to more cohesion and increased resistance to indentation due to the micro load. The magnesium oxide (MgO) constitutes 65% and nickel (Ni) 35%. The increase in temperature level causes a decrease in porosity while there is an increase in density, which means that there is a reduction in areas of weakness in the sample, and also the resistance of the surface to penetration increases. This explains the increase in Vickers hardness when the temperature levels rise. From the results obtained from the hardness test, it can be deduced that the process of sintering was successful since the packing and bonding of the grains in the MgO-Ni composition increased.

Table 4. Vickers hardness results for the prepared compound.

Degree of sintering (°C)	Hard Viker (HV)
700	301.7
800	314.9
900	333.6
1000	349.2
1100	367.8

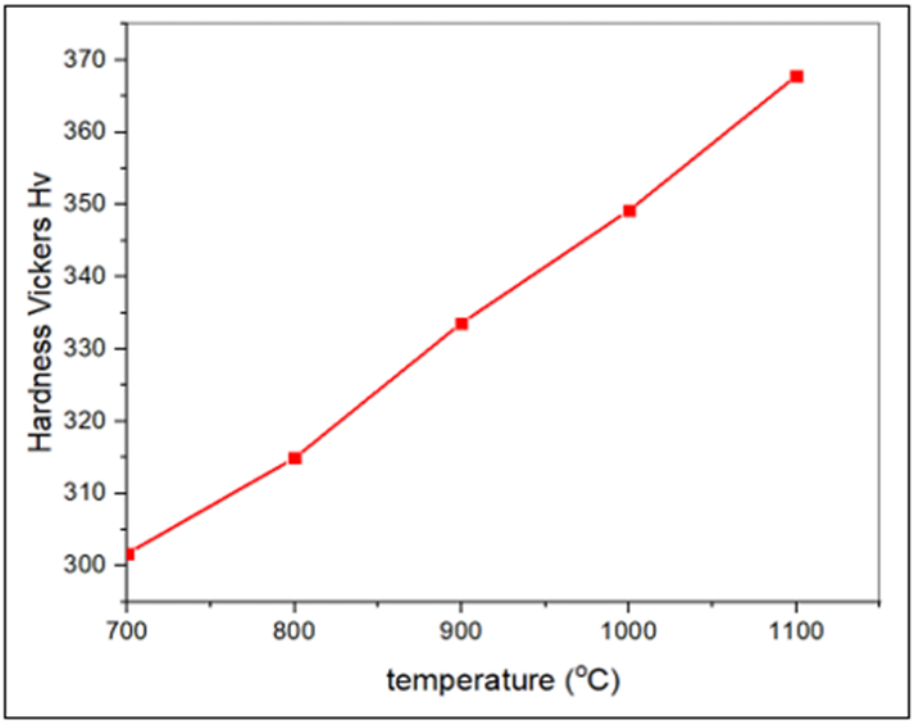

Figure 3. Sintering temperatures versus Vickers hardness of the prepared composite.

2. Compressive strength

The compressive strength results for the composite compacts shown in Fig (4) and Table (5) indicate a change in compressive strength values as the sintering temperature increases from °C (700 to 1100), with values ranging between MPa (320.8 and 339.6) This behaviour reflects that the chemical composition of the material is stable and that the effect of sintering is limited to improving the internal structure without causing a radical change in the compressive strength mechanism. The gradual increase in compressive strength is due to improved intergranular bonding and a reduction in residual porosity within the sintered bodies, which reduces stress concentration under compressive loading. However, this improvement remains within limited bounds due to the stability of the ceramic and metallic phase ratios, with MgO remaining the primary deformation-resistant component, whilst Ni contributes to improved cohesion without a significant change in overall mechanical behaviour. Furthermore, stronger interparticle bonds at higher sintering temperatures improve stress transfer within the structure; however, the absence of a change in composition or the emergence of new phases means that the effect of sintering temperature is gradual rather than abrupt. This behaviour is desirable in practical terms, as it indicates good mechanical stability of the material across a wide range of sintering temperatures. These results suggest that the MgO–Ni composite possesses relatively stable compressive strength, making it suitable for applications requiring mechanical stability under compressive loads, with the potential to partially improve performance by controlling the sintering degree without the need to alter the composition.

Table 5. Compressive strength results for a composite.

Degree of calcification (°C)	Compressive strength (MPa)
700	320.8
800	326.1
900	332.9
1000	336.4
1100	339.6

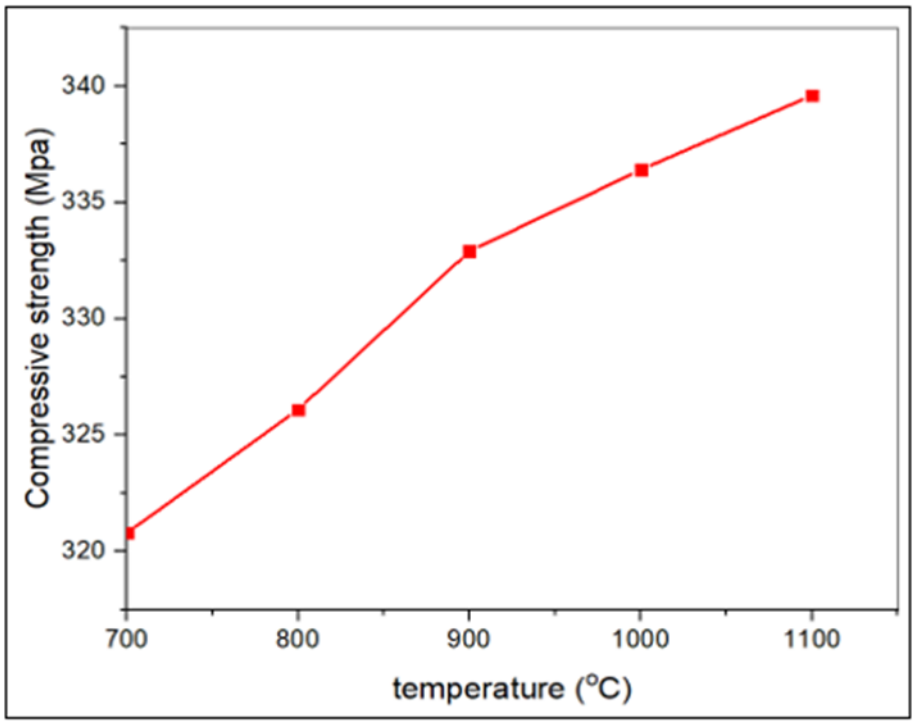

Figure 4. Sintering temperatures versus compressive strength of the prepared composite.

3. Wear

The results of the wear test on the composite shown in Figure 5 revealed a marked reduction in the wear rate as the sintering temperature increased from 700 to 1100°C. This behaviour indicates an improvement in the surface's resistance to wear as a result of the structural and microstructural changes that occur during the sintering process, as shown in Table (6). The reduction in the wear rate is directly related to an increase in Vickers hardness and an improvement in the cohesion of the composite's microstructure, as higher sintering temperatures reduce porosity and increase intergranular bonding; this helps to minimise the detachment of surface particles during friction, thereby limiting material loss and reducing the wear rate. The nature of the composite's constituents also plays an important role in this behaviour; MgO provides high wear resistance due to its hard, ceramic nature, whilst Ni enhances cohesion and localised ductility, which helps to absorb part of the stresses generated during friction and reduces the formation of surface cracks. The balanced interaction between these two phases leads to improved wear performance of the composite. These results demonstrate that controlling sintering conditions contributes to improving the wear resistance of the MgO –Ni composite, making it suitable for engineering applications requiring high durability and effective resistance to friction, such as mechanical components subjected to continuous loads and sliding.

Table 6. Wear tests.

Degree of calcification (°C)	Average of Wear ($\times 10^{-4}$ mm³/N ·m)
700	6.82
800	5.97
900	5.21
1000	4.56
1100	3.98

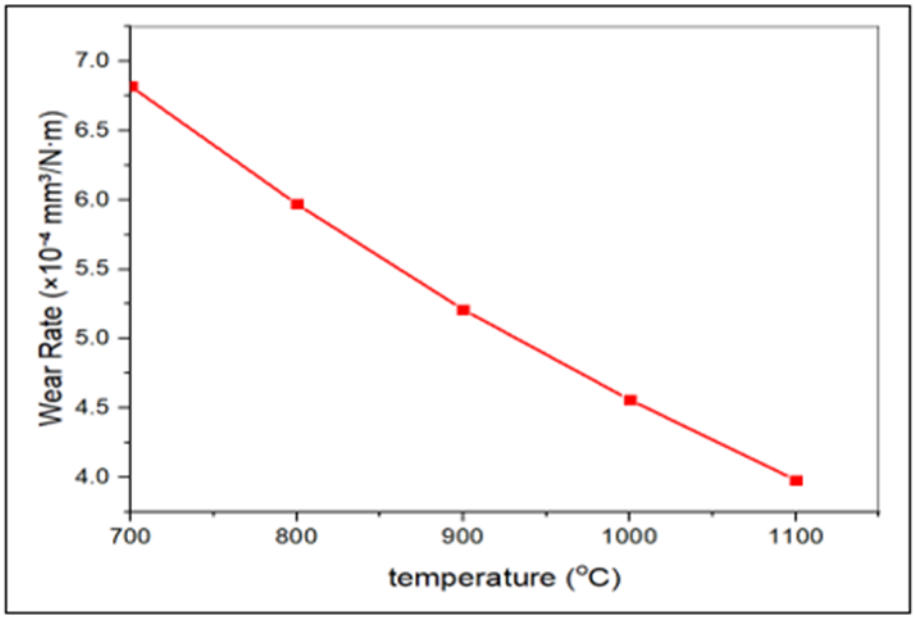

Figure 5. Calcination temperatures versus wear rate.

CONCLUSION

Fundamental Finding : Following the results discussed, the tests, the first of which was X-ray diffraction, showed that the MgO -Ni compound has a stable phase at low temperatures without the appearance of secondary phases, whilst the intensity varies within a crystal volume that differs according to the Miller indices. From this, we demonstrate that temperature has a clear effect on the crystal structure. Furthermore, the scanning electron microscopy image shows that the compound has a homogeneous structure and that there is a clear increase in crystal size with increasing calcination. Hardness also increases with rising temperature, which improves intergranular bonding and reduces porosity; this appears to be a positive correlation. It is noted that the strength remains stable, indicating consistent mechanical behaviour with increasing temperature. The wear rate decreases as temperature rises, which is consistent with the increase in hardness and improvement in structure. **Implication :** Finally, it can be said that the composite has demonstrated excellent results in the tests, which confirms its suitability for promising applications, particularly in the engineering industries. **Limitation :** This study is limited to the evaluation of the MgO-Ni composite under a specific range of calcination temperatures and preparation conditions. Therefore, the findings may not fully represent the behavior of the composite under different sintering durations, heating

rates, MgO-Ni composition ratios, or manufacturing methods. The characterization was primarily based on X-ray diffraction, scanning electron microscopy, hardness, strength, and wear tests. At the same time, other important properties, such as fracture toughness, thermal conductivity, corrosion resistance, oxidation behavior, and long-term thermal stability, were not examined. In addition, the study did not include direct performance testing under actual engineering operating conditions. These limitations restrict the generalization of the results to broader industrial applications. **Future Research :** Future research should investigate a wider range of calcination temperatures, sintering durations, heating rates, and MgO-Ni composition ratios to determine the optimum processing conditions for achieving superior structural and mechanical properties. Further studies are also recommended to evaluate fracture toughness, thermal conductivity, corrosion resistance, oxidation resistance, fatigue behavior, and long-term stability under elevated temperatures. Advanced characterization techniques may be employed to examine phase distribution, grain boundaries, elemental composition, and interfacial bonding in greater detail. In addition, comparative studies using alternative preparation and sintering methods should be conducted. Future research should also include prototype development and testing under actual engineering conditions to confirm the composite's suitability for high-temperature, wear-resistant, and high-hardness industrial applications.

REFERENCES

[1] Srivastava, R., & Yadav, B. C. (2012). Ferrite materials: introduction, synthesis techniques, and applications as sensors. International Journal of Green Nanotechnology, 4(2), 141-154.

[2] Kefeni, K. K., Mamba, B. B., & Msagati, T. A. (2017). Application of spinel ferrite nanoparticles in water and wastewater treatment: a review. Separation and Purification Technology, 188, 399-422.

[3] Hemeda, O. M., Tawfik, A., Mostafa, M., Zaki, M., & Abd El Ati, M. I. (2019, June). Structural and magnetic properties of nano ferrite for magnetoelectric applications. In Journal of Physics: Conference Series (Vol. 1253, No. 1, p. 012026). IOP Publishing.

[4] Galindo, R., Menendez, N., Crespo, P., Velasco, V., Bomati-Miguel, O., Díaz-Fernández, D., & Herrasti, P. (2014). Comparison of different methodologies for obtaining nickel nanoferrites. Journal of magnetism and magnetic materials, 361, 118-125.

[5] Al-Hadad, S. H. A., & Sulaiman, S. H. (2015). Structural and electric investigations of Al-doped nano nickel ferrite. Engineering and Technology Journal, 33(3 Part (B) Scientific).

[6] Hezam, F. A., Khalifa, N. O., Nur, O., & Mustafa, M. A. (2021). Synthesis and magnetic properties of $Ni_{0.5}Mg_xZn_{0.5-x}Fe_2O_4$ ($0.0 \leq x \leq 0.5$) nanocrystalline spinel ferrites. Materials Chemistry and Physics, 257, 123770.

[7] Al-Rawi, N. N., Anwer, B. A., Al-Rawi, N. H., Uthman, A. T., & Ahmed, I. S. (2020). Magnetism in drug delivery: The marvels of iron oxides and substituted ferrites nanoparticles. Saudi Pharmaceutical Journal, 28(7), 876-887.

[8] Dhiman, P., Kumar, A., Rana, G., & Sharma, G. (2023). Cobalt–zinc nanoferrite for synergistic photocatalytic and peroxymonosulfate-assisted degradation of sulfosalicylic acid. Journal of Materials Science, 58(24), 9938-9966.

[9] Madhu, B. J., Ashwini, S. T., Shruthi, B., Divyashree, B. S., Manjunath, A., & Jayanna, H. S. (2014). Structural, dielectric and electromagnetic shielding properties of Ni–Cu nanoferrite/PVP composites. Materials Science and Engineering: B, 186, 1-6.

[10] Gamal, W. M., El-Bassuony, A. A. H., Abdelsalam, H. K., & Wahab, S. A. E. (2021). Role of elastic and optical properties on silver nanoferrite and nanochromite for optical switch device applications. Journal of Materials Science: Materials in Electronics, 32, 21590-21602.

[11] Koomson, V. J., & Afsar, M. N. Design and Fabrication of Millimeter--wave Integrated Circuits Using Hexagonal Nanoferrite Materials.

[12] Mkwae, P. S., Kortidis, I., Kroon, R. E., Leshabane, N., Jozela, M., Swart, H. C., & Nkosi, S. S. (2020). Insightful acetone gas sensing behaviour of Ce substituted $MgFe_2O_4$ spinel nano-ferrites. Journal of Materials Research and Technology, 9(6), 16252-16269.

[13] Mazurkiewicz, M., Rhee, C. K., & Weglinski, B. (2008). Magnetic Powder and Nano-powder Composites for Electrical Converters. Journal of Powder Materials, 15(4), 320-330.

[14] Alkhazaali, H. K. G. (2021, July). Study the electrical and magnetic properties of Ferrite $Ni_{1-x}Zn_xFe_2O_4$ films and their potential use in the magnetic core of transformers. In Journal of Physics: Conference Series (Vol. 1963, No. 1, p. 012031). IOP Publishing.

[15] Ega, C. S., Babu, B. R., Ramesh, K. V., Sreenivasulu, M., & Purushotham, Y. (2019). Correlation between structural, magnetic and dielectric properties of microwave sintered Ni-Zn-Al nanoferrites. Journal of Superconductivity and Novel Magnetism, 32, 3525-3534.

[16] Li, H., Zhu, K., Lei, K., Xu, T., & Wu, H. (2022). Integrated MEMS toroidal transformer with Ni-Zn ferrite core for power supply on chip. IEEE Transactions on Power Electronics, 37(9), 10075-10080.

[17] Gao, Y., Wang, Z., Pei, J., & Zhang, H. (2019). Structural, elastic, thermal and soft magnetic properties of Ni-Zn-Li ferrites. Journal of Alloys and Compounds, 774, 1233-1242.

[18] Niu, X., Zong, B., Hu, H., & Wu, B. (2017). Influence of Sn^{4+}-substituted on the magnetic properties and power loss of Ni-Zn soft magnetic ferrites. Optik, 134, 135-139.

[19] Macrelli, E., Romani, A., Wang, N., Roy, S., Hayes, M., Paganelli, R. P., ... & Tartagni, M. (2014). Modeling, design, and fabrication of high-inductance bond wire microtransformers with toroidal ferrite core. IEEE Transactions on Power Electronics, 30(10), 5724-5737.

[20] Manikandan, A., Antony, S. A., Sridhar, R., Ramakrishna, S., & Bououdina, M. (2015). A simple combustion synthesis and optical studies of magnetic $Zn_{1-x}Ni_xFe_2O_4$ nanostructures for photoelectrochemical applications. Journal of nanoscience and nanotechnology, 15(7), 4948-4960.

***Dheyab T. Noori (Corresponding Author)**
Ministry of Higher Education and Scientific Research, Tikrit University, College of Education - Tuz Khurmatu, Iraq
Email: theyab.thair.tuz@tu.edu.iq